ACUSTICA · acta acustica
Vol. 86 (2000) 216–228

Elastic Moduli and Dissipative Properties of Microinhomogeneous Solids with Isotropically Oriented Defects

V. Zaitsev*, P. Sas
Katholieke Universiteit Leuven, Mechanical Engineering Department, Celestijnenlaan 300 B, B-3001, Heverlee, Belgium

Summary
Elastic properties and sound absorption in a solid containing isotropically oriented highly compliant microinhomogeneities are theoretically analysed. The suggested model describing microinhomogeneous media can be applied to a wide class of materials, such as rocks, concretes and other solids with similar microinhomogeneous structure. Using the model, expressions for the elastic moduli, the Poisson ratio and the decrements for the longitudinal, the Young (rod) and the transversal elastic waves in isotropic microinhomogeneous materials are derived. Inter-relations of the microstructure of the solid, its elastic and dissipative properties are analysed. The results allow for prediction of the absorption in the material and of the complementary change of its elastic parameters without detailed knowing of viscoelastic properties of the defects. The obtained conclusions are shown to be in a good agreement with existing phenomenological theoretical approximations and with known experimental data on elasticity/attenuation in rocks and in some other microstructured solids.

PACS no. 43.20.Hq, 43.20.Ir, 43.35.Cg, 91.60.Lj

1. Introduction

Materials with microinhomogeneous structure have been attracting ever-increasing interest to study their acoustic properties which are significantly different from the ones typical for homogeneous samples of amorphous solids and single crystals [1, 2, 3, 4, 5, 6, 7, 8, 9, 10, 11, 12, 13, 14, 15]. This refers to a very wide class of apparently different materials such as rocks, concrete and similar construction materials, grainy media, polycrystalline metals, etc. Seemingly, recently synthesized nano-crystalline solids [16] can also be put in the same class. Those media in many cases are characterized by anomalously high elastic nonlinearity compared to the above mentioned "normal" homogeneous solids. In addition, in the same microinhomogeneous materials, elastic wave dissipation is also significantly increased in magnitude, while functionally their absorption coefficient is approximately proportional to the frequency in contrast to the quadratic-in-frequency law typical for "normal" viscous absorption.

Recently, a series of papers was published [17, 18, 19, 20, 21] in which the mentioned elastic and dissipative properties were considered in the framework of an instructive model of a microinhomogeneous solid. Those anomalous properties appeared to be consistently explained as complementary manifestations of material micro-defects which are significantly softer compared to the surrounding intact matrix material. The models [17, 18, 19, 20, 21] allowed for explanation of main features of the phenomena and made it possible to determine the relation between the material microstructure and the acoustic properties of the medium. In these papers, however, the models were considered in 1D approximation, although the theoretical approach itself based on the energy balance was not essentially restricted to the 1D-case. Therefore, the results derived in these works were qualitatively valid for real materials also, although numerical estimates are applicable to the 3D case only with an accuracy within an order of magnitude. Besides, some essentially volumetric features (for example, the difference between the Young modulus and the elastic modulus for the bulk longitudinal wave, and the difference between the corresponding decrements) could not be accounted for in the 1D approximation.

In this paper, the theoretical approach and the microinhomogeneous medium model suggested in [17, 18, 19, 20, 21] are generalized for the 3D case. However, here we restrict our consideration to the linear approximation in order to analyze the absorption of elastic wave energy in an isotropic microinhomogeneous medium for different types of waves as well as to determine the change of the material elastic moduli and the Poisson ratio.

2. Main features of the material structure and the defect properties

In the present consideration, the main qualitative features of the model of microinhomogeneous media suggested in [17, 18, 19, 20, 21] are conserved. Namely, it was already noted that microinhomogeneous solids always posses some microstructure (grains, cracks, etc.) with a characteristic scale which is larger than the atomic size, but small compared to the acoustic wavelength [17, 20]. It is essential that in many cases the mentioned defect-inclusions are much softer than the surrounding defect-free material, whereas the compliance of the inclusions being ranged over a rather wide band. At a given stress, due to the high compliance of the defects, their local strain (and the velocity of strain changes) is much higher compared to the mean strain (and strain velocity) of the medium. Consequently, both the dissipation of

Received 16 August 1999,
accepted 17 February 2000.

* Also at the Institute of Applied Physics RAS, 46 Uljanova Str., Nizhny Novgorod, 603600, Russia

the wave and the volume density of the elastic energy are significantly (by several orders of magnitude) increased at the defects compared to the surrounding homogeneous and more rigid material. That is why even a small density of such defects can change pronouncedly the mean acoustical properties of the material. This leads to a series of interesting conclusions on linear and nonlinear elastic, dispersive and dissipative properties of microinhomodeneous materials even in the 1D representation of the model of the medium (see details in references [17, 18, 19, 20, 21]). In order to provide more rigorous accounting for features of real solids, let us specify now the defect properties implied in the 3D model.

It is essential that the soft defect-inclusions in a solid can be considered as some planar (disk-like) objects, which can correspond, for example, to real cracks with the nearest layer of adjacent intact material (see Figure 1). The planar geometry of the discontinuity-like defects is necessary to provide their high compliance. Indeed it is well known that in "normal" solids (whose Poisson's ratio γ is not very close to the "liquid" limit $\gamma = 0.5$ typical for a special class of the so-called rubber-like materials), the effective compressibility of near-spherical cavities is of the same order of magnitude as the compressibility of the intact matrix material [8, 10]. However, planar defects can be strongly compliant in normal solids (metals and rocks) with the Poisson ratio $\gamma < 0.4 \ldots 0.45$ [1, 2, 8, 10].

When stress is applied along the axis normal to the defect plane (see Figure 1a), the defect deformation in this normal direction (change of the defect thickness X_n) can be related to the applied stress via an effective elastic modulus $E_d \equiv \zeta E$, where E is the Young modulus of the matrix material, and $\zeta \ll 1$ is the parameter of the defect compliance in the normal direction. By definition, the compliance parameter ζ belongs to the interval $0 \leq \zeta \leq 1$. If the area of a disk-like defect is equal to S and its thickness is $L \ll \sqrt{L}$, then the normal component of stress σ_n in terms of the introduced notations is related to the variation of the thickness by the following equation:

$$S\sigma_n = E_d \frac{S}{L} X_n \equiv \zeta E \frac{S}{L} X_n. \tag{1}$$

Therefore the elastic energy accumulated by each defect due to the work of the normal stress is given by:

$$W_i^{(n)} = \int_0^{X_n} S\sigma_n \, \mathrm{d}X_n = \frac{SL\sigma_n^2}{2\zeta E} = \frac{V_i \sigma_n^2}{2\zeta E}. \tag{2}$$

Here $V_i = SL$ is the defect volume. Note that due to the high compliance of the defect with respect to normal stress, the density of stored elastic energy is sharply increased compared to that stored in the surrounding intact material. In case of in-plane compression (see Figure 1b) the situation is different. Namely, a volume of a material containing a planar defect is significantly more rigid with respect to in-plane compression compared to the case of normal stress. The defect strain due to compression in the in-plane direction is much smaller

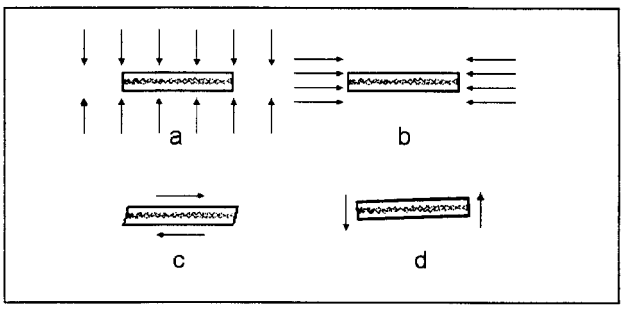

Figure 1. Schematically shown a disc-shape (planar) defect under the action of applied stress. (a) – normal compression; (b) – in-plane compression; (c) – in-plane shear stress; (d) – shear stress in normal direction.

(of the same order of magnitude as in the intact material). Therefore, we can neglect the corresponding elastic energy stored by the defect compared to the amount of the elastic energy accumulated by the same defect due to its normal deformation, which is described by equation (2).

To illustrate the above formulated properties one can take an instructive example of a penny-like cut (crack) whose deformation under a normal stress is considered, for example, in reference [22]. According to the results presented in [22], for such a defect its parameter of compliance ζ can be written as:

$$\zeta = \frac{d_0}{R} \frac{3\pi}{16(1-\gamma^2)}, \tag{3}$$

where d_0 is the opening of the crack, R is its radius, and γ is the Poisson ratio for the matrix material. For example, for a very thin micro-crack with an opening of about a typical atomic size $d_0 = 3 \cdot 10^{-4}\,\mu$m (which is actually the minimal physically possible opening) and the crack's radius $R = 10 \ldots 30\,\mu$m, one readily gets the estimate $\zeta = (1 \ldots 3) \cdot 10^{-5}$ for the matrix material with a typical value of $\gamma = 0.25 \ldots 0.4$. Similar small values of the compliance parameter are readily obtained for larger (in both dimensions) cracks in rocks. This estimate also indicates that for natural cracks with randomly ranged ratios d_0/R it is reasonable to expect that the corresponding parameters of compliance widely range from the above estimated small magnitudes up to the values comparable to the rigidity of the matrix material. Similar estimates can be obtained [19] for inter-granular contacts of the Hertz type, or, in other cases (e.g., for defects at inter-grain boundaries in polycrystalline solids or complex-shape cracks), the effective parameters of defect compliance can be introduced phenomenologically.

Following such a way, we can write that when a soft defect is under the action of a shear stress in the in-plane direction (see Figure 1c), the corresponding relation of the applied tangential shear stress σ_τ to the defect deformation X_τ in the tangential direction has the form similar to equation (1):

$$S\sigma_\tau = G_d \frac{S}{L} X_\tau \equiv \xi G \frac{S}{L} X_\tau. \tag{4}$$

The notations are also similar to those in equation (1), $G_d = \xi G$, where G_d is the effective shear modulus of the

ACUSTICA · acta acustica
Vol. 86 (2000)

defect, G is the shear modulus (the Lame coefficient) of the matrix material, and is the effective parameter of shear compliance of the defect. It is reasonable to expect that in some cases (for example, for inter-granular contacts or large enough cracks with diameter much greater than the thickness), the shear compliance of the defects can be significantly reduced ($\xi \ll 1$). However, for smaller planar defects, probably only the normal compliance is significantly increased ($\zeta \ll 1$), while their shear compliance remains close to that of the intact material. Then, by analogy with (2), for a defect which is subjected to shear in-plane stress and which is highly compliant in this direction, the amount of accumulated elastic energy is given by the expression:

$$W_i^{(\tau)} = \int_0^{X_\tau} S\sigma_\tau \, \mathrm{d}X_\tau = \frac{SL\sigma_\tau^2}{2\xi G} = \frac{V_i\sigma_\tau^2}{2\xi G}. \qquad (5)$$

When a shear stress is applied along the axis transversal to the defect plane (Figure 1d), the defect shape remains practically unperturbed and it rather tends to rotate as a whole (like a piece of intact material), so the amount of own elastic energy of the defects in such a case can be neglected compared to the value given by equation (5).

The above mentioned properties and the corresponding parameters determine the elastic response of the defects to different types of applied stress, which is implied in the model. It should be added also that the defects are supposed to be isotropically oriented in the material, so that the material itself should be considered as average-isotropic within volumes containing large amount of defects. Another important assumption is that the defects are separated by distances that are significantly larger than the defect diameter. This condition allows one to consider the stress applied to a defect as given and makes it possible to neglect the perturbations caused by other defects. The characteristic spatial scale of the average stress field (i.e., the length of an elastic wave) is supposed to be also significantly larger that the inter-defect distance.

The described model of a microinhomogeneous medium is evidently applicable to a wide class of initially intact solids (like rocks or metals) with a small amount of crack-like defects, however, it cannot be directly applied to the case of non-consolidated (crumbly) materials similar to sand. Let us consider first mean elastic properties of a solid material containing defects-inclusions with the described properties.

3. Elastic properties of the microinhomogeneous material

In order to characterize linear elastic properties of an isotropic material it is sufficient to know two of its elastic parameters, for example, the modulus K of its compressibility at uniform (hydrostatic) pressure and its Young modulus corresponding to the case of uniaxial stress [23]. These moduli determine the volume density $W_{\mathrm{el.}}$ of elastic energy of the material under the action of the corresponding type of stress. In this paper we shall restrict our analysis to the linear approximation and shall use the energy approach which in papers [17, 18, 19, 20, 21] was used for the derivation of both linear and nonlinear elastic parameters in 1D approximation. However it is necessary to take into account specific features of the 3D case. Namely, at the uniform pressure, when the stress tensor $\sigma_{ik} = \delta_{ik}\sigma$, the expression for the volume density of the elastic energy in the material has the following form:

$$W_{\mathrm{el.}} = \frac{\sigma^2}{2K}, \qquad (6)$$

where K is the modulus of volume compressibility.

At the uniaxial stress, when the components of the stress tensor are $\sigma_{zz} = \sigma$, $\sigma_{xx} = \sigma_{yy} = 0$, $\sigma_{i\neq k} = 0$, the energy density is determined by a similar equation:

$$W_{\mathrm{el.}} = \frac{\sigma^2}{2E}, \qquad (7)$$

where E is the Young modulus. When the medium is microinhomogeneous the mean energy density $\langle W_{\mathrm{el.}} \rangle$ can be described by similar expressions with some effective moduli $K_{\mathrm{eff.}}$ and $E_{\mathrm{eff.}}$ which are influenced by the occurrence of the defects:

$$\langle W_{\mathrm{el.}} \rangle = \frac{\sigma^2}{2K_{\mathrm{eff.}}}, \quad \text{or} \quad \langle W_{\mathrm{el.}} \rangle = \frac{\sigma^2}{2E_{\mathrm{eff.}}}. \qquad (8)$$

On the other hand, the mean energy density in a microinhomogeneous material can be calculated directly by summation of amounts of the elastic energy stored at all defects and in the matrix material per unit volume of the medium. Comparison of equations (8) with the formulae obtained by such a direct summation should give the effective values of elastic moduli expressed via elastic parameters of the matrix material and the parameters of the defects and their volume content.

To determine the elastic energy stored at the defects it is necessary to calculate normal and tangential stress components σ_n and σ_τ acting on the defects at the uniform compression and at the uniaxial stress and then to use equations (2) and (4).

The case of the uniform compression is the simplest. When the stress tensor $\sigma_{ik} = \delta_{ik}\sigma$, the normal stress component is equal for all defects: $\sigma_n = \sigma$. Therefore, in order to calculate the mean energy density it is possible to substitute directly $\sigma_n = \sigma$ in equation (2) for the contribution of the defects and to use equation (5) for the energy density in the matrix material. Summation of these contributions yields:

$$\langle W_{\mathrm{el.}} \rangle = \frac{(1 - v_t)\sigma^2}{2K} + \frac{\sigma^2}{2E} \int \frac{v(\zeta)}{\zeta} \, \mathrm{d}\zeta, \qquad (9)$$

where $v(\zeta)$ is a distribution function of the defects over their compliance, so that the amount $v(\zeta)\mathrm{d}\zeta$ characterizes the relative volume content (their volume per unit volume of the material) of arbitrary oriented defects whose parameter of the normal compliance belongs to the region $[\zeta, \zeta + \mathrm{d}\zeta]$. Therefore the value $v_t = \int v(\zeta)\mathrm{d}\zeta$ corresponds to the total volume of all defects contained in a unit volume of the

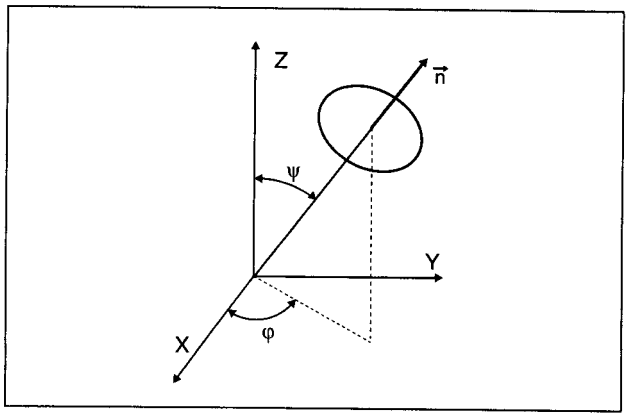

Figure 2. Spatial orientation of a defect.

microinhomogeneous material. Note that exactly in the same way the distribution $v(\xi)$ over another (shear) compliance parameter can be introduced for the volume content of defects with any spatial orientation (see Figure 2) and any parameter ζ. In general case, the defects should be characterized by their distribution $v(\psi, \varphi, \zeta, \xi)$ over both elastic parameters ζ, ξ, and the angles ψ, φ, of defect spatial orientation (see Figure 2). Distribution $v(\psi, \varphi, \zeta, \xi)$ should be normalized to the total volume content of all defects v_t in the conventional sense:

$$v_t = \int_0^{2\pi} \mathrm{d}\varphi \int_0^{\pi} \int_0^1 \int_0^1 v(\psi, \varphi, \zeta, \xi) \sin\psi \, \mathrm{d}\psi \, \mathrm{d}\zeta \, \mathrm{d}\xi, \quad (10)$$

so that the distributions $v(\zeta)$ and $v(\xi)$ over elastic parameters ζ, ξ, correspond to:

$$v(\zeta) = \int_0^{2\pi} \mathrm{d}\varphi \int_0^{\pi} \int_0^1 v(\psi, \varphi, \zeta, \xi) \sin\psi \, \mathrm{d}\psi \, \mathrm{d}\xi, \quad (11)$$

$$v(\xi) = \int_0^{2\pi} \mathrm{d}\varphi \int_0^{\pi} \int_0^1 v(\psi, \varphi, \zeta, \xi) \sin\psi \, \mathrm{d}\psi \, \mathrm{d}\zeta. \quad (12)$$

It is important that the distributions over elastic parameters and the distribution $v(\psi, \varphi)$ over spatial orientations are essentially independent, so it is possible to perform averaging over defect orientations independently for defects with different elastic parameters. In case of isotropic orientations, the uniform angular distribution $v(\psi, \varphi)$ should be normalized as:

$$v(\psi, \varphi) = \frac{1}{4\pi} \quad (13)$$

in order to be consistent with equations (10) through (12).

Note that parameter ξ of the shear compliance was not significant for the case of the uniform compression, but it could be important in the case of the uniaxial stress, when the components of the stress tensor are $\sigma_{zz} = \sigma$, $\sigma_{xx} = \sigma_{yy} = 0$, $\sigma_{i \neq k} = 0$. In this case, both the stress component normal to the defect plane and the tangential stress component should be taken into account, their values being dependent on the orientation of the defect. Therefore, in the notations introduced in Figure 2, the normal and the tangential stress components are given by the equations

$$\sigma_n = \sigma \cos^2\psi, \quad (14)$$

$$\sigma_\tau = \sigma \cos\psi \sin\psi. \quad (15)$$

These values have to be substituted in equations (2) and (4) for the elastic energies of the defects. The summation of shares of defects with isotropic orientations to the total elastic energy of the material, therefore, corresponds to averaging the values σ_n^2 and σ_τ^2 over the uniform angular distribution:

$$\langle \sigma_n^2 \rangle = \int_0^{2\pi} \mathrm{d}\varphi \int_0^{\pi} \sigma_n^2(\psi, \varphi) v(\psi, \varphi) \sin\psi \, \mathrm{d}\psi = \frac{1}{4\pi} \int_0^{2\pi} \mathrm{d}\varphi \int_0^{\pi} \sigma_n^2(\psi, \varphi) \sin\psi \, \mathrm{d}\psi, \quad (16)$$

$$\langle \sigma_\tau^2 \rangle = \int_0^{2\pi} \mathrm{d}\varphi \int_0^{\pi} \sigma_\tau^2(\psi, \varphi) v(\psi, \varphi) \sin\psi \, \mathrm{d}\psi = \frac{1}{4\pi} \int_0^{2\pi} \mathrm{d}\varphi \int_0^{\pi} \sigma_\tau^2(\psi, \varphi) \sin\psi \, \mathrm{d}\psi, \quad (17)$$

where $\sigma_n^2(\psi, \varphi)$ and $\sigma_\tau^2(\psi, \varphi)$ are given by expressions (14), (15) in the considered case.

Taking into account relations (14) through (17), the summation for defects with isotropic orientations gives the following equation for the mean elastic energy at uniaxial stress:

$$\langle W_{\mathrm{el.}} \rangle = \frac{(1 - v_t)\sigma^2}{2E} + \frac{1}{5}\left(\frac{\sigma^2}{2E}\right) \int \frac{v(\zeta)}{\zeta} \mathrm{d}\zeta + \frac{2}{15}\left(\frac{\sigma^2}{2G}\right) \int \frac{v(\xi)}{\xi} \mathrm{d}\xi. \quad (18)$$

Comparison of equations (8) with equation (9) for the uniform compression, and with equation (18) for the uniaxial stress, readily yields for the effective moduli:

$$K_{\mathrm{eff.}} = K\left[(1 - v_t) + \frac{K}{E} \int \frac{v(\zeta)}{\zeta} \mathrm{d}\zeta\right]^{-1}, \quad (19)$$

$$E_{\mathrm{eff.}} = E\left[(1 - v_t) + \frac{1}{5} \int \frac{v(\zeta)}{\zeta} \mathrm{d}\zeta + \frac{2E}{15G} \int \frac{v(\xi)}{\xi} \mathrm{d}\xi\right]^{-1}. \quad (20)$$

Expressions (19), (20) are direct generalizations of similar equations for the effective elastic modulus obtained earlier [17, 18, 19] for 1D medium models. However, now additional effects of shear deformation of the defects and the distribution of the defects over all orientations within the spatial angle are taken into account.

Below we shall neglect the term v_t in equations (9), (18) and in their consequencies (19) and (20) because the inequal-

ACUSTICA · acta acustica
Vol. 86 (2000)

ities

$$v_t = \int v(\zeta)\,\mathrm{d}\zeta \ll \int \frac{v(\zeta)}{\zeta}\,\mathrm{d}\zeta,$$
$$v_t = \int v(\xi)\,\mathrm{d}\xi \ll \int \frac{v(\xi)}{\xi}\,\mathrm{d}\xi$$

are valid for highly compliant defects with compliance parameters $\zeta, \xi \ll 1$, and the defect concentration is rather small $v_t \ll 1$ (as we supposed that the distance between the defects is much greater than their size).

Further, it is possible to apply conventional relationships [23] between the elastic moduli and the Poisson ratio for an isotropic medium. Then equations (19) and (20) readily yield the following expressions for the effective value of the Poisson ratio $\gamma_{\text{eff.}}$ and for the relative change (for example, $\tilde{E} = E_{\text{eff.}}/E$, etc.) of the elastic moduli:

$$\gamma_{\text{eff.}} = \frac{\gamma - \frac{1}{15}N_1 + \frac{2}{15}(1+\gamma)N_2}{1 + \frac{1}{5}N_1 + \frac{4}{15}(1+\gamma)N_2}, \tag{21}$$

$$\tilde{E} = \frac{E_{\text{eff.}}}{E} = \frac{1}{1 + \frac{1}{5}N_1 + \frac{4}{15}(1+\gamma)N_2}, \tag{22}$$

$$\tilde{G} = \frac{G_{\text{eff.}}}{G} = \frac{1}{1 + \frac{2}{15}N_1/(1+\gamma) + \frac{2}{5}N_2}, \tag{23}$$

$$\tilde{M} = \frac{M_{\text{eff.}}}{M} = \left[1 + \frac{\frac{4}{15}N_1}{1-\gamma} + \frac{\frac{2}{15}N_2(1+\gamma)}{(1-\gamma)}\right] \cdot \left[1 + \frac{\frac{2}{15}N_1}{1+\gamma} + \frac{2}{5}N_2\right]^{-1}\left[1 + \frac{\frac{1}{3}N_1}{1-2\gamma}\right]^{-1}. \tag{24}$$

Here γ is the Poisson ratio for the matrix material, and notations M and $M_{\text{eff.}}$ are introduced for the moduli corresponding to the longitudinal bulk wave in the medium without defects (the matrix material) and in the microinhomogeneous medium, respectively.

Parameters N_1 and N_2 in expressions (21) through (24) have the following meaning:

$$N_1 = \int \frac{v(\zeta)}{\zeta}\,\mathrm{d}\zeta, \quad N_2 = \int \frac{v(\xi)}{\xi}\,\mathrm{d}\xi. \tag{25}$$

In case of identical defects with fixed values of compliance parameters ζ and ξ, the distributions have the form of delta-functions, so that:

$$N_1 = \frac{v_t}{\zeta}, \qquad N_2 = \frac{v_t}{\xi}. \tag{26}$$

Physically, as it is clear from equations (25), (26), parameters N_1 and N_2 are determined jointly by the compliance of the defects and their concentration. Further, as it was argued above, it is natural to assume that real defects are characterized by a wide distribution over their parameters of compliance, and it is convenient to approximate the distributions by wide Π-shape functions (by analogy with papers [19, 20, 21]):

$$v(\zeta) = \begin{cases} v_0^{(1)}, & \text{when } \zeta \in [a_1, b_1],\ a_1 \ll b_1 \ll 1, \\ 0, & \text{when } \zeta \notin [a_1, b_1], \end{cases} \tag{27}$$

and

$$v(\xi) = \begin{cases} v_0^{(2)}, & \text{when } \xi \in [a_2, b_2],\ a_2 \ll b_2 \ll 1, \\ 0, & \text{when } \xi \notin [a_2, b_2]. \end{cases} \tag{28}$$

Therefore,

$$v_t = \int_0^1 v(\zeta)\,\mathrm{d}\zeta = (b_1 - a_1)v_0^{(1)} \approx b_1 v_0^{(1)}, \tag{29a}$$

and

$$v_t = \int_0^1 v(\xi)\,\mathrm{d}\xi = (b_2 - a_2)v_0^{(2)} \approx b_2 v_0^{(2)}. \tag{29b}$$

Parameters N_1 and N_2 then have the following forms:

$$N_1 = v_t \frac{\ln(b_1/a_1)}{b_1}, \qquad N_2 = v_t \frac{\ln(b_2/a_2)}{b_2}. \tag{30}$$

It can be noted that parameter N_2 may be either smaller (for rigid in shear direction defects) or comparable, or even higher than N_1. Therefore, depending on the relation of parameters N_1 and N_2, the effective Poisson ratio in the medium with soft defects can be either greater or smaller than in the homogeneous matrix material (according to equation (21), the total range for $\gamma_{\text{eff.}}$ is determined by the inequality $-1/3 < \gamma_{\text{eff.}} < 1/2$). It is interesting to note, that the Poisson ratio $\gamma_{\text{eff.}}$ can even become negative at

$$N_1 > 15\gamma + 2(1+\gamma)N_2,$$

which (according to equations 25–30) can be reached at yet small total concentration $v_t \ll 1$ of highly compliant defects. Unlike the Poisson ratio (which can either decrease or increase) the elastic moduli in a medium with soft inclusions will always decrease according to equations (22) through (24). However, the relative rate of the decrease of different moduli depends essentially on the properties of the defects via the relation of parameters N_1 and N_2. For different values of ratio N_1/N_2, the decrease in values of the shear, longitudinal or the Young moduli can be significantly different. We consider in details the corresponding examples in the following sections.

4. Absorption in the microinhomogeneous medium

In order to calculate absorption of the elastic waves we apply an energy-balance approach in the form similar to the one used in paper [20]. It is convenient to derive the non-dimensional decrement θ which is related to the wave absorption coefficient α as $\theta = \alpha\lambda = \alpha C/f$, where λ is the wavelength of an elastic wave, f is its frequency, and C is its velocity. The same decrement can be also expressed via the ratio

$$\theta = \frac{W_{\text{dis.}}}{2W_{\text{el.}}}, \tag{31}$$

where $W_{\text{dis.}}$ means the wave energy losses in a unit volume during one period of a harmonic wave, and $W_{\text{el.}}$ is the

maximal value of density of the elastic energy of the wave motion.

In equation (31), the density of the elastic energy is given by expressions (8) for the bulk longitudinal wave and for the rod (Young) wave, and by the similar equation for the shear wave with the effective shear modulus $G_{\text{eff.}}$ instead of the effective moduli $K_{\text{eff.}}$ and $E_{\text{eff.}}$ in equations (8).

In order to calculate the losses $W_{\text{dis.}}$, it is necessary to take into account that the defects are characterized not only by their elastic coefficients, but also by effective viscosity corresponding to the dissipation of the elastic energy at the defects. Physically, this dissipation can be attributed, for example, to thermal losses caused by increased temperature gradients [23] and increased material compression in the vicinity of the defects either at compressional or at shear defect deformation [24]. In both cases there should occur material compression due to complex distribution of stress in the nearest vicinity of a defect. The losses due to both types of defect deformation (compressional or shear) contribute to the total value of the decrement and can be estimated independently.

4.1. Absorption due to compressional deformation of the defects

Let us first consider the losses caused by normal compression of the soft defects. Introducing coefficient g_1 for the effective viscosity of the defects into their equation of state under normal compression we obtain a generalization of equation (2):

$$S\sigma_n = E_d \frac{S}{L} X_n + g_1 \frac{\mathrm{d}X_n}{\mathrm{d}t} \equiv \zeta E \frac{S}{L} X_n + g_1 \dot{X}_n, \qquad (32)$$

where $\mathrm{d}X_n/\mathrm{d}t \equiv \dot{X}_n$. The mean power of the elastic energy dissipation is proportional to the period-averaged value $\langle g_1 \dot{X}_n^2 \rangle \sim \omega^2 g_1 |X_n|^2$, where $\omega = 2\pi f$ is the wave angular frequency and the amplitude $|X_n|$ is related to the normal component σ_n of the elastic stress via equation (32).

The normal component of stress, in its turn, depends on the defect orientaion and on the type of applied stress. In case of the uniaxial stress (longitudinal rod wave) it is determined by expression (14), $\sigma_n = \sigma T_1(\psi, \varphi) = \sigma \cos^2 \psi$. In case of a longitudinal wave or for a transversal wave, the angular coefficient $T_1(\psi, \varphi)$ can be found in a similar manner considering the normal projections of the corresponding stresses. Further, performing the averaging of σ_n^2 according to equation (16), which corresponds to the summation of the dissipation at all defects with different spatial orientations (but identical compliance parameter ζ), one obtains the following expression for the "compressional" decrement $\theta^{(1)}(\omega, \zeta)$:

$$\theta^{(1)}(\omega, \zeta) = \pi v(\zeta) \frac{D_{\text{eff.}}}{E} \langle T_1^2(\varphi, \psi) \rangle \frac{\omega/\Omega_1}{\zeta^2 + (\omega/\Omega_1)^2}. \qquad (33)$$

In equation (33), coefficient $D_{\text{eff.}}$ corresponds to the effective value of a particular elastic modulus (for example, $M_{\text{eff.}}$ for the bulk longitudinal or $G_{\text{eff.}}$ for the transversal wave) for which expressions (22) through (24) were derived in the previous section. The characteristic relaxation frequency Ω_1 introduced in equation (33) depends on the effective viscosity of the defects:

$$\Omega_1 = \frac{ES}{g_1 L}. \qquad (34)$$

The angular coefficient $\langle T^2(\varphi, \psi) \rangle$ is determined by the averaging the squared normal stress component (for the corresponding type of the stress field) over spatial orientaions of the defects. The averaging procedure is similar to the one in the previous section and gives:

$$\left\langle T_1^2(\varphi, \psi) \right\rangle = \qquad (35)$$
$$\begin{cases} \dfrac{1}{5} + \dfrac{2\gamma_{\text{eff.}}}{15(1-\gamma_{\text{eff.}})} + \dfrac{8}{15} \dfrac{\gamma_{\text{eff.}}^2}{15(1-\gamma_{\text{eff.}})^2} & \text{for the bulk longitudinal wave,} \\ \dfrac{1}{5} & \text{for the rod (Young) wave,} \\ \dfrac{1}{15} & \text{for the transversal wave.} \end{cases}$$

The value of the Poisson ratio $\gamma_{\text{eff.}}$ of the microinhomogeneous material is determined by equation (21).

Further, we should take into account the distribution $v(\zeta)$ of the defects over their compliance and make the corresponding summation by analogy with the consideration of the elastic moduli in the previous section. It is reasonable again to use the Π-shape distribution function (27). Then the summation (integration of equation (33) over $\mathrm{d}\zeta$) yields:

$$\theta^{(1)}(\omega) = \pi v_0^{(1)} \frac{D_{\text{eff.}}}{E} \left\langle T_1^2(\varphi, \psi) \right\rangle \arctan\left(\frac{\zeta}{\omega/\Omega_1}\right)\Big|_{a_1}^{b_1}. \qquad (36)$$

Concerning the frequency behaviour of the decrement, the most intersting consequence which follows from this equation is that in a wide frequency band

$$a_1\Omega_1 < \omega < b_1\Omega_1, \qquad (37)$$

the difference $\arctan(b_1\Omega_1/\omega) - \arctan(a_1\Omega_1/\omega) \approx$ const. $= \pi/2$, and, therefore, decrement $\theta^{(1)}(\omega)$ is practically independent of the frequency ω of the wave, and, moreover, the decrement value in this frequency band does not depend on the effective viscosity of the defects. Actually this means that the implicit assumption of equal effective viscosity of the defects (or rather the assumption of a constant value of the relaxation frequency Ω_1) was not necessary for the validity of the above-formulated conclusion. This result was discussed in more details in papers [20, 21] in which the model of the microinhomogeneous medium was one-dimensional.

Therefore, in the wide frequency band $a_1\Omega_1 < \omega < b_1\Omega_1$, the decrement $\theta^{(1)}(\omega)$ is approximately constant ($\theta^{(1)}(\omega) = \theta_c^{(1)}$ =const.), and equation (36) provides a reasonable estimate for the absorption magnitude using only

ACUSTICA · acta acustica
Vol. 86 (2000)

the parameters of the elastic properties of the defects and their volume content:

$$\theta_c^{(1)} = \frac{\pi^2}{2} v_0^{(1)} \frac{D_{\text{eff.}}}{E} \left\langle T_1^2(\varphi,\psi) \right\rangle \approx \frac{\pi^2}{2} \frac{v_t}{b_1} \frac{D_{\text{eff.}}}{E} \left\langle T_1^2(\varphi,\psi) \right\rangle. \quad (38)$$

In terms of the above introduced parameter N_1 and the normalized non-dimensional moduli $\tilde{D} = D_{\text{eff.}}/D$, it is possible to rewrite expression (38) also in the following unified form:

$$\theta_c^{(1)} = \frac{\pi^2}{2} v_0^{(1)} \tilde{D} \frac{D}{E} \left\langle T_1^2(\varphi,\psi) \right\rangle \approx \frac{\pi^2}{2} \frac{N_1}{\ln(b_1/a_1)} \tilde{D} \frac{D}{E} \left\langle T_1^2(\varphi,\psi) \right\rangle. \quad (39)$$

Thus via expressions (21) through (24), the decrement value is related to the effective normalized moduli $D_{\text{eff.}}$ and to the Poisson parameters γ_{eff} and γ of the microinhomogeneous medium and of the matrix material.

4.2. Absorption due to shear deformation of the defects

Let us turn to the consideration of the absorption of the considered types of the elastic waves caused by shear deformation of the soft defects. We denote the corresponding decrements as $\theta^{(2)}(\omega)$ by analogy with contribution $\theta^{(1)}(\omega)$ due to the compressional deformation of the defects. It is clear from the analysis in the previous section, that the maximal value of the decrement $\theta^{(1)}(\omega)$ in the frequency band (37) does not depend on the effective viscosity itself, and, according to expressions (38) and (39), it is essentially determined by the geometrical and elastic parameters of the defects. Therefore, even if the parameters of the effective defect viscosity at normal compression and at shear deformation are significantly different, the maximal values of the corresponding shares $\theta_c^{(1)}$ and $\theta_c^{(2)}$ to the total decrement $\theta(\omega)$ can be comparable in magnitude. However, the corresponding characteristic frequency bands $[a_1\Omega_1, b_1\Omega_1]$ for $\theta_c^{(1)}(\omega)$ and $[a_2\Omega_2, b_2\Omega_2]$ for $\theta_c^{(2)}(\omega)$ can be either overlapped or essentially separated in the frequency domain. Therefore, for a wave with a given frequency, these mechanisms may act either simultaneously or essentially separately, depending on the defects properties.

In case of shear deformation of the defects, effective parameter g_2 of the "shear" viscosity can be introduced by analogy with equation (32):

$$S\sigma_\tau = G_d \frac{S}{L} X_\tau + g_2 \frac{\mathrm{d}X_\tau}{\mathrm{d}t} \equiv \xi G \frac{S}{L} X_\tau + g_2 \dot{X}_\tau. \quad (40)$$

Then losses due to effective viscosity at shear deformation can be estimated in the same manner as for the case of compression. The main distinction is that in this case it is necessary to take into account not normal, but tangential projection σ_τ of the elastic stress. Doing so, one obtains the expression for the share of the defects with all orientations, but fixed parameter ξ of shear compliance:

$$\theta^{(2)}(\omega,\xi) = \pi v(\xi) \frac{D_{\text{eff.}}}{G} \left\langle T_2^2(\varphi,\psi) \right\rangle \frac{\omega(\Omega_2}{\xi^2 + (\omega/\Omega_2)^2}. \quad (41)$$

By analogy with equation (33), in equation (41), coefficient $D_{\text{eff.}}$ corresponds to the effective value of a particular elastic modulus ($E_{\text{eff.}}$, $M_{\text{eff.}}$ or $G_{\text{eff.}}$) for the corresponding wave type (the rod longitudinal wave, the bulk longitudinal wave or the shear wave). The characteristic frequency Ω_2 in equation (41) depends on the effective viscosity of the defects at shear deformation:

$$\Omega_2 = \frac{GS}{g_2 L}. \quad (42)$$

Angular coefficient $\langle T_2^2(\varphi,\psi)\rangle$ for the tangential projection is determined by the averaging (over the spatial orientaions of the defects) the squared tangential stress component σ_τ^2 for the corresponding type of the wave field. The averaging procedure which is similar to the one in the previous sections gives:

$$\left\langle T_2^2(\varphi,\psi) \right\rangle = \begin{cases} \frac{2}{15}\left(\frac{1-2\gamma_{\text{eff.}}}{1-\gamma_{\text{eff.}}}\right)^2 & \text{for the bulk longitudinal wave,} \\ \frac{2}{15} & \text{for the rod (Young) wave,} \\ \frac{4}{15} & \text{for the transversal wave.} \end{cases} \quad (43)$$

Summation of the shares of all defects with different shear compliance ξ over the distribution (29) then yields the following expression for the "shear" decrement $\theta^{(2)}(\omega)$:

$$\theta^{(2)}(\omega) = \pi v_0^{(2)} \frac{D_{\text{eff.}}}{G} \left\langle T_2^2(\varphi,\psi) \right\rangle \arctan\left(\frac{\xi}{\omega/\Omega_2}\right)\Big|_{a_2}^{b_2}. \quad (44)$$

In the frequency band $a_2\Omega_2 < \omega < b_2\Omega_2$, by analogy with equation (38), again the decrement is approximately constant and close to its maximal value:

$$\theta_c^{(2)} = \frac{\pi^2}{2} v_0^{(2)} \frac{D_{\text{eff.}}}{G} \left\langle T_2^2(\varphi,\psi) \right\rangle \approx \frac{\pi^2}{2} \frac{v_t}{b_2} \frac{\tilde{D}}{G} \left\langle T_2^2(\varphi,\psi) \right\rangle. \quad (45)$$

In terms of parameter N_2 and the normalized moduli $\tilde{D} = D_{\text{eff.}}/D$ by analogy with equation (39) it can be rewritten as:

$$\theta_c^{(2)} = \frac{\pi^2}{2} v_0^{(2)} \tilde{D} \frac{D}{G} \left\langle T_2^2(\varphi,\psi) \right\rangle \approx \frac{\pi^2}{2} \frac{N_2}{\ln(b_2/a_2)} \tilde{D} \frac{D}{G} \left\langle T_2^2(\varphi,\psi) \right\rangle. \quad (46)$$

All the qualitative features mentioned in the discussion of the decrement $\theta^{(1)}(\omega)$ are valid for $\theta^{(1)}(\omega)$ as well. Total decrement $\theta(\omega)$ is determined by the sum of the both shares:

$$\theta(\omega) = \theta^{(1)}(\omega) + \theta^{(2)}(\omega). \quad (47)$$

Expressions (39), (46) for the decrements $\theta^{(1)}$ and $\theta^{(2)}$ contain effective defect densities $N_{1,2}$ as well as the relative

widths $b_{1,2}/a_{1,2}$ of the defect distributions over their elastic parameters. However, this ratio is under the logarithmic function, and, therefore, even quite a large uncertainty within an order of magnitude in the estimate of the ratio, for example, $b_{1,2}/a_{1,2} \approx 10^3 \ldots 10^4$ gives only an uncertainty of 20% in the calculation of the decrements.

Note further, that parameters N_1 and N_2 in expressions (39), (46) for the decrements can be estimated from experimental data on variation $\Delta D/D$ of the elastic moduli using equations (22) through (24). The latter expressions were derived in the quasi-static limit that corresponds to frequencies $\omega \ll a_{1,2}\Omega_{1,2}$ for which the viscous terms in equations (32), (40) can be neglected. For higher frequencies, however, the microstructure-induced perturbations $\Delta D/D$ of the elastic moduli are frequency dependent due to the influence of the defects viscosity. This dependence (which can be derived, for example, using the Kramers-Kronig relations and the expression for the decrement) was considered in paper [21] in the 1D approximation. The results obtained there are also approximately applicable to the discussed 3D case. It was shown that inside the band $a\Omega < \omega < b\Omega$ (here we omit indexes 1, 2), the microstructure-induced perturbation $\Delta D/D$ of the elastic modulus is characterized by a logarithmic dispersion:

$$\frac{\Delta D(\omega)}{D} \approx 2\frac{\Delta C(\omega)}{C} \propto v_0 \ln \frac{b^2 + (\omega/\Omega)^2}{a^2 + (\omega/\Omega)^2}, \quad (48)$$

where $C(\omega) = \sqrt{D(\omega)/\rho}$ is the wave velocity, and ρ is the medium density. Within frequency band $a\Omega < \omega < b\Omega$, where the decrement θ (or the corresponding quality factor $Q = \pi/\theta$) is approximately constant ($Q \approx \pi/\theta_c$ =const.), equations (27), (38) and (28), (46) allow to re-write dispersion relation (48) in the following form:

$$\frac{C(\omega_1)}{C(\omega_2)} \approx 1 + \frac{1}{\pi Q} \ln \frac{\omega_1}{\omega_2}. \quad (49)$$

Note that numerous experimental data give exactly this logarithmic form of the approximation for the frequency dependence of wave velocity in solids with the almost constant quality factor [25, 26]. This agreement with the known experimental data on the dispersion provides an additional argument that the considered model gives realistic predictions of the wave properties. In this paper, however, we are focused not on the dispersion, but on the evaluation of the microstructure-induced absorption and on the complementary decrease of the elastic moduli. Therefore, in the examples considered below we neglect the dispersional correction and compare the values of the decrements with the corresponding variations (22), (23), (24) of the elastic moduli which are found in the quasistatic (low-frequency) approximation. Such a comparison provides quite a reasonable evaluation for the almost constant decrement in the frequency band $a\Omega < \omega < b\Omega$. Indeed, in this frequency band, one can use the quasi-static estimate $\ln(b/a)$ for the logarithm in equation (48) with an uncertainty of a factor about two. However, if necessary, the dispersion correction in the form (48) can be applied to the quasi-static equations (22) through (24) for the variations of the elastic moduli.

5. Discussion

The analysis performed in the previous sections shows that the presence of soft micro- defects in an intact solid results in increase of the absorption and in simultaneous reduction of the effective moduli of the microinhomogeneous material. The relative decrease of the different elastic moduli depends on the ratio of the parameters N_1 and N_2 which, in turn, depend on the elastic properties of the defects and on the defect volume content via expressions (25), (29), (30). It was shown also that the Poisson ratio can either decrease or increase depending on the compliance of the planar defects with respect to normal or shear applied stress.

It is reasonable to distinguish the following characteristic cases: $N_1/N_2 \gg 1$, $N_1/N_2 \sim 1$, and $N_1/N_2 \ll 1$. When relation $N_1/N_2 \gg 1$, the defects are highly compliant only with respect to a normal stress. When both the normal and the shear compliances are comparable, the ratio is $N_1/N_2 \sim 1$. Finally, when the shear compliance is higher, the following inequality is valid: $N_1/N_2 \ll 1$.

The corresponding examples of calculation of the decrease of the elastic moduli, the variation of the Poisson ratio and the corresponding maximal values of decrements $\theta_c^{(1)}$ and $\theta_c^{(2)}$ are plotted in Figures 3 and 4 against parameter N_1 proportional to the defect content. Figure 3 corresponds to the "compressional" decrement $\theta_c^{(1)}$, and in Figure 4, the "shear" decrement $\theta_c^{(2)}$ is shown. These examples demonstrate that when $N_1/N_2 \gg 1$, the decrease is the highest for the elastic modulus for the bulk longitudinal wave (see Figures 3a and 4a). The Poisson ratio in this case pronouncedly decreases with increase of the defect content. When $N_1/N_2 \sim 1$, all elastic moduli decrease approximately with the same rate (see Figures 3b and 4b), and, correspondingly, the Poisson ratio remains almost unperturbed. Finally, when $N_1/N_2 \ll 1$, the decrease of the modulus for the bulk longitudinal wave is the smallest (Figures 3c and 4c), whereas the Poisson ratio pronouncedly increases.

Concerning the absorption, comparison of Figures 3 and 4 shows that the compressional and the shear deformation of the defects cause different relative dissipation magnitudes for different types of waves. Namely, "compressional" decrement $\theta_c^{(1)}$ is the largest for the bulk longitudinal wave and is the smallest for the transversal wave (see Figure 3), whereas "shear" decrement $\theta_c^{(2)}$ instead can be significantly larger for the transversal wave compared to those for the bulk longitudinal wave (see Figures 4a and 4b). Note, that such essentially different cases were really observed for seismic waves. Experiments indicate, for example, that in different kinds of rocks the decrement for the longitudinal wave can be either greater or smaller than for the transversal wave [3].

Figures 3 and 4 give also an impression on the magnitude of the change in elastic moduli $\tilde{D} = \tilde{D}(N_1)$ and on the corresponding magnitude of the decrements, $\theta_c^{(1)}(N_1)$ and $\theta_c^{(2)}(N_1)$ for the plane longitudinal, the Young (rod) wave and the transversal wave. The figures show that decrease in the velocity of the longitudinal wave by 10... 25% (compared to the intact matrix material) corresponds, for ex-

ACUSTICA · acta acustica
Vol. 86 (2000)

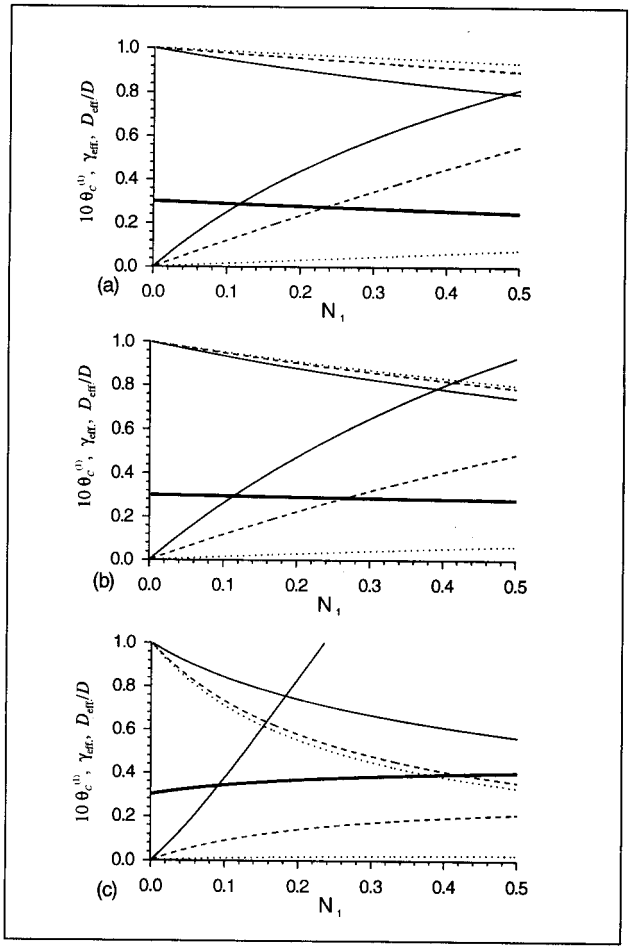

Figure 3. Examples of calculated dependencies of the "compressional" decrement, the Poisson ratio and the variation of the elastic moduli on parameter N_1. The middle thick line in the plots is the Poisson ratio. Upper thin curves are for the normalized elastic moduli $\tilde{D} = D/D_{\text{eff.}}$; the lower curves are for the corresponding decrements, $10\theta_c^{(1)}$; the solid thin lines (——) being for the longitudinal wave; the dashed lines (– – –), for the Young (rod) wave, and the dotted lines (·····), for the transversal wave. Poisson's ratio for the matrix material $\gamma = 0.3$; ratio of parameters $b_1/a_1 = b_2/a_2 = 3 \cdot 10^3$, parameters $b_{1,2} = 3 \cdot 10^3$. (a) – ratio $N_1/N_2 = 10$, (b) – ratio $N_1/N_2 = 1$, (c) – ratio $N_1/N_2 = 0.1$.

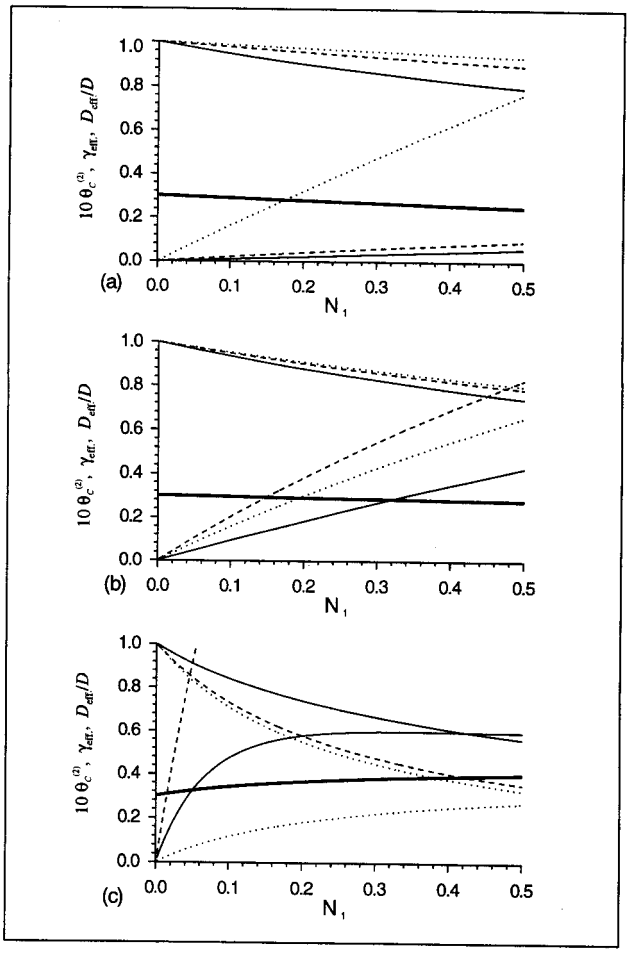

Figure 4. Examples of calculated dependencies of the "shear" decrement, the Poisson ratio and the variation of the elastic moduli on parameter N_1. The middle thick line in the plots is the Poisson ratio. Upper thin curves are for the normalized elastic moduli $\tilde{D} = D/D_{\text{eff.}}$; the lower curves are for the corresponding decrements, $10\theta_c^{(2)}$; the solid thin lines (——) being for the longitudinal wave; the dashed lines (– – –), for the Young (rod) wave, and the dotted lines (·····), for the transversal wave. Poisson's ratio for the matrix material $\gamma = 0.3$; ratio of parameters $b_1/a_1 = b_2/a_2 = 3 \cdot 10^3$, parameters $b_{1,2} = 3 \cdot 10^3$. (a) – ratio $N_1/N_2 = 10$, (b) – ratio $N_1/N_2 = 1$, (c) – ratio $N_1/N_2 = 0.1$.

ample, to the decrement $\theta_c^{(1)}(N_1) \sim (3 \ldots 8) \cdot 10^{-2}$, which is unusually high for homogeneous media (like amorphous defect-free glass or single crystals), but instead is typical for such microinhomogeneous solids as rocks [3, 24, 25, 26, 27]. For the comparison with the model, it is important to stress that numerous experimental data on attenuation in rocks indicate that the decrement typically is almost constant in a wide frequency band [3, 25, 26, 27, 28], which agree well with the obtained results on the frequency behaviour of the decrements (see equations (36), (44) and their discussions). Besides rocks, similar increased absorption and the almost constant quality factor is also typical for many polycrystalline metals whose properties are also essentially determined by microstructural inter-grain defects [28].

Note further, that the model not only predicts the existence of the relatively wide frequency bands $[a_1\Omega_1, b_1\Omega_1]$ and $[a_2\Omega_2, b_2\Omega_2]$ in which partial decrements $\theta_c^{(1)}(\omega)$ and $\theta_c^{(2)}(\omega)$ are almost constant, but provides a more detailed description. It was already mentioned that, in the general case, the respective position of the characteristic bands $[a_1\Omega_1, b_1\Omega_1]$ and $[a_2\Omega_2, b_2\Omega_2]$ can be arbitrary: they may either overlap or be essentially separated in the frequency domain. Therefore, the dependence on frequency of the resultant decrement $\theta(\omega) = \theta_c^{(1)}(\omega) + \theta_c^{(2)}(\omega)$ in these cases can be more complex and significantly different (either decrease or increase) at different frequency ranges and for different types of waves. Examples plotted in Figure 5 demonstrate qualitatively the frequency behavior of the partial and the total decrements for the longitudinal and the transversal waves in case when, for example, the interval $[a_2\Omega_2, b_2\Omega_2]$ is lower in frequency than interval $[a_1\Omega_1, b_1\Omega_1]$. Namely, the following parameters are chosen: $b_1/a_1 = b_2/a_2 = 3 \cdot 10^3$,

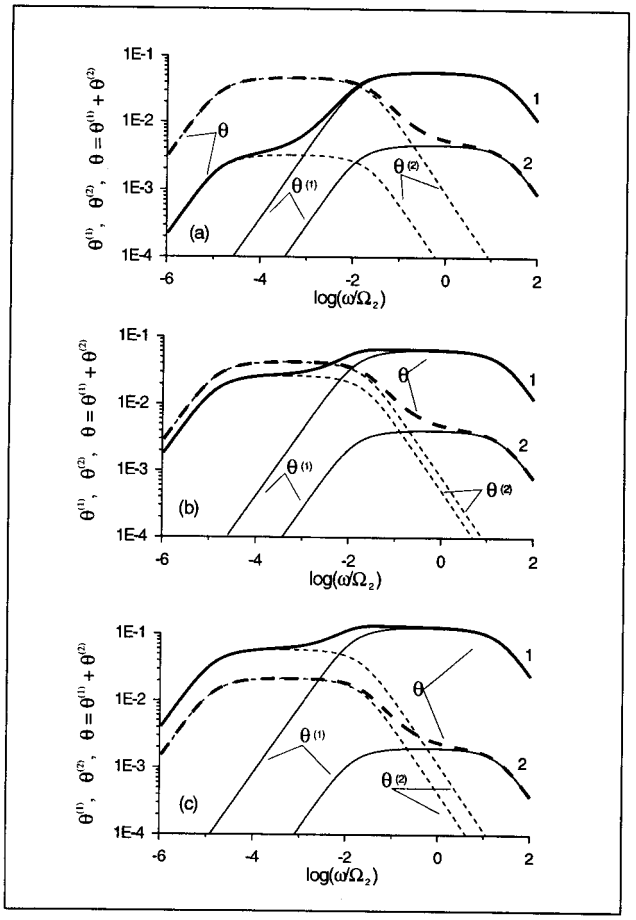

Figure 5. Examples of frequency behavior of absorption. The thin solid curves are for ("compressional" decrement $\theta^{(1)}(\omega)$, the dashed curves are for "shear" decrement $\theta^{(2)}(\omega)$, and the thick curves are for the resultant decrement $\theta(\omega) = \theta^{(1)}(\omega) + \theta^{(1)}(\omega)$. Number 1 is for the longitudinal wave, number 2 is for the transversal wave. Poisson's ratio for the matrix material $\gamma = 0.3$; parameter $N_1 = 0.3$, ratio $b_{1,2}/a_{1,2} = 3 \cdot 10^3$, $b_{1,2} = 0.03$, ratio $\Omega_1/\Omega_2 = 10^3$. (a) – ratio $N_1/N_2 = 10$, (b) – ratio $N_1/N_2 = 1$, (c) – ratio $N_1/N_2 = 0.1$.

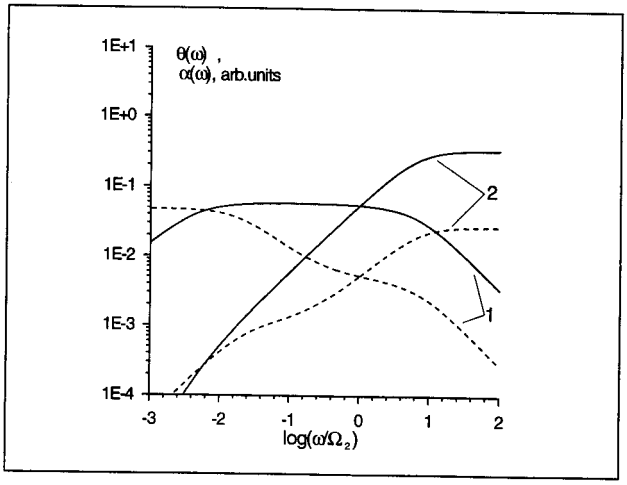

Figure 6. An example of the frequency behavior for the decrement $\theta(\omega) = \theta^{(1)}(\omega) + \theta^{(1)}(\omega)$, (lines marked by 1), and for the absorption coefficient $\alpha(\omega) \propto \omega\theta(\omega)$, (lines marked by 2). The solid curves are for longitudinal and the dotted curves are for transversal waves. The relation $N_2 = N_1/10$, initial Poisson's ratio $P = 0.3$; parameter $N_1 = 0.3$; ratio of parameters $b_1/a_1 = b_2/a_2 = 3{\cdot}10^3$; ratio $\Omega_1/\Omega_2 = 300$.

$\Omega_1/\Omega_2 = 10^3$, and the effective density $N_1 = 0.3$ (the corresponding values of the elastic moduli can be readily found by comparison with Figures 3, 4). Corresponding values of ratio N_1/N_2 are indicated in the figure caption. Figure 5 demonstrates that the ratio of the microstructure-induced decrements for the transversal and the longitudinal waves can either increase or decrease with frequency or can remain almost constant depending on the parameters of the microinhomogeneous material.

Another example plotted in Figure 6 shows qualitatively the frequency behaviors of the full decrements $\theta(\omega) = \theta_c^{(1)}(\omega) + \theta_c^{(2)}(\omega)$ and the corresponding absorption coefficients $\alpha(\omega) = \omega\theta(\omega)/(2\pi C)$ for the longitudinal and transversal waves when interval $[a_2\Omega_2, b_2\Omega_2]$ for the "shear" absorption mechanism is positioned lower than interval $[a_1\Omega_1, b_1\Omega_1]$ for the "compressional" mechanism. The logarithmic scale is equal for both axes to show directly the power exponents of the dependencies via the slope of the corresponding curves. Figure 6 demonstrates an interesting case of essentially different frequency dependencies for the absorption coefficients for the longitudinal and the transversal waves. Namely, in the wide frequency band (from -2 to 0 in the non-dimensional logarithmic scale) the absorption coefficient for the longitudinal waves increases almost linearly with frequency (solid curve 2), whereas the dependence for the absorption coefficient of the transversal wave is pronouncedly slower (dotted curve 2). The slope of the latter curve changes from approximately 0.5 to 1 in the considered frequency range. This example demonstrates that the same structural mechanism of absorption can cause significantly different frequency dependencies for attenuation of different types of waves.

Note that along with rocks and some polycrystalline metals, the above obtained results probably can be also relevant to nano-crystalline metals, for which the absorption coefficient is anomalously high in magnitude and is approximately linearly proportional to ultrasound frequency, whereas the sound velocities (elastic modules) are significantly (by 10...20%) lower compared to the same metals in the "normal" polycrystalline state [16]. The latter fact indicates clearly that there is a significant amount of highly compliant microinhomogeneities in the material structure, which is the basic property of the considered model. It can be stated that qualitatively, the measured functional dependencies in experiments [16] correspond fairly well to the obtained above results. In particular, almost constant quality factor was also observed in the nanocrystalline materials and even an example of different frequency dependencies for the longitudinal and for the transversal waves was reported in [16] for the same frequency range (see the discussion of Figure 6 above). Moreover, even quantitative estimates of the absorption based on the experimental data on the decreased elastic moduli and on the derived equations (39),

ACUSTICA · acta acustica
Vol. 86 (2000)

(46) for the decrements give the magnitudes of the decrement $\theta_c \sim (3 \ldots 9) \cdot 10^{-2}$ which are close to the reported experimental data. On the other hand, according to the estimations performed in [16], this strong attenuation exhibited by the nanocrystalline samples could not be attributed to presently known mechanisms alone.

Concerning the comparison of the results of this paper with existing models, it can be pointed out that the obtained dependencies are in a good agreement with known phenomenological approximations describing experimental results on elastic waves velocities and attenuation in many microinhomogeneous solids. In particular, a rather comprehensive phenomenological model describing velocities and attenuation of seismic waves was developed by Gurevich [29] on the basis of thorough systematization of numerous experimental data (the summary of the main results originally published in [29] can be more easily found in review [3]). The central point of this model was the hypothesis that the approximately constant quality factor of rocks and the logarithmic dispersion could be attributed to a wide spectrum of classical exponential-type relaxation processes whose spectral density is proportional to the characteristic relaxation frequency. Later on, other authors also considered similar relaxation-band models [30, 31] which allowed for fairly well fitting the known variety of experimental data on seismic wave absorption and dispersion [25, 26]. However, the physical meaning of these phenomenologically introduced relaxation processes and the connection of the parameters of these models to the medium microstructure remained unknown [3, 26]. In principle, the almost-constant decrement could be phenomenologically approximated by alternative ways, for example, using the only one relaxation process with a non-exponential kernel of the form t^{-m}, $0 < m < 1$ (e.g., [26, 32] and analogous recent works [33, 34]). However, the question about a plausible physical interpretation of these phenomenological kernels also remains to be open [26, 33, 34]. In this context, the model derived in the present paper can be considered as a physical argument in favor of the exponential relaxation-band hypotheses [29, 30, 31], as the above performed consideration provides physical insight in the nature of these hypothetical relaxation processes and directly relates them with microstructural features of microinhomogeneous solids.

Concerning other non-phenomenological models it can be noted that they mostly considered separately either the elastic properties of microinhomogeneous solids ([1, 2] and similar later models, e.g., [35, 36, 37]) or the attenuation caused by nonlinear (e.g., frictional) mechanisms [28, 38, 39, 40], as it seemed impossible to obtain the almost constant quality factor in models based on conventional linear viscous-like losses. It may be shown that the mentioned mutually consistent results [1, 2, 35, 36, 37] obtained for elastic properties of solids with cracks and based on particular models of cracks are also consistent with the above obtained inferences on the material elastic properties. By appropriately re-formulating key parameters N_1 and N_2 in terms of notations used in those works the above derived equations (19) through (24) may be reduced to concrete cases considered in [1, 2, 35, 36, 37]. For example, expressions for the elastic moduli obtained in works [35, 36] in case of dry elliptical cracks correspond to equations (19) through (24) when the crack's density (in the notations of [35, 36]) is equal to $(3/16)N_1/(1-\gamma^2)$, whereas the ratio $N_1/N_2 = (1+\gamma)(2-\gamma^2)$. The latter ratio characterizes relative importance of the defect compliance in the normal and tangential directions, and the value $N_1/N_2 = (1+\gamma)(2-\gamma^2)$ is specific of the particular model of dry elliptical cracks, which was used in [1, 2, 35, 36].

Therefore, in terms of the analysis performed above, the dry elliptical cracks are evidently close to the case $N_1/N_2 \approx 1$ (see the corresponding plots for the elastic moduli and the decrements in Figures 3b, 4b and 5b). However, as it is pointed in [37], almost no cracks in situ are ellipsoidal cavities, and other models of cracks may exhibit noticeably different elastic properties. Consequently, ratio N_1/N_2 may be noticeably different for different types of cracks. The influence of such variations of the normal and tangential compliance of the defects can be readily analyzed in the framework of the suggested approach (in fact, the results of such analysis are presented in the examples of plots corresponding to different values of N_1/N_2 in Figures 3 through 5). Further, as it was argued in papers [35, 36], presence of a fluid in a crack may significantly affect its elastic properties, namely, the normal stiffness of the crack may significantly increase, whereas in the tangential direction the crack remains highly compliant. Such fluid-saturated defects which are highly compliant only in the tangential direction, in terms of parameters N_1 and N_2, correspond to the case $N_1/N_2 \ll 1$. Therefore, the above obtained results on material elasticity and dissipation in case of $N_1/N_2 \ll 1$ may be interpreted as being pertinent to fluid-saturated cracked solids. Such a comparison indicates that, in combination with particular models of defects (like those used in [1, 2, 35, 36, 37]), the suggested approach may be developed to effectively account for the cases of either dry or partially and completely fluid-saturated microinhomogeneous solids.

Another important example of a self-consistent micromechanical description of both the elasticity and the attenuation is the wide group of models of porous media based on Biot's ideas [26, 41, 42]. However, in these models the wave absorption was attributed only to the interaction of the solid matrix with flows of a porous gas or a liquid, and dissipation associated with the mineral frame was not included in the micromechanical consideration. The Biot model does not give the almost constant decrement and predicts the attenuation coefficient that depends on frequency f, scaling as f^2 at low frequencies and as $\sqrt{f}$ above some threshold frequency, which has a limited application to real rocks [28].

Concerning the losses in the solid skeleton, it is essential to note that experimental data on attenuation in dry porous rocks indicate that the observed differences should be predominantly connected with some fine microstructural features of the solid skeleton, rather than with the macroscopic properties such as density or porosity [28, 43]. The model of Biot [37, 38] and its modifications [26, 28] cannot account for this fact as they do not consider own attenuation in the solid matrix. On the other hand, this experimentally established

weak dependence on the macroscopic porosity appears to be in a good agreement with the model suggested here. To illustrate this, one can make an estimate using, for example, the material parameters accepted for the calculations presented in Figure 3a. Then it follows from expression (38) that the typical for rocks decrement $\theta = 6 \cdot 10^{-2}$ (or in terms of the quality factor $Q = \pi/\theta \approx 50$) corresponds to the total specific volume content of the soft microcracks $v_t \approx 2 \cdot 10^{-3}$. Such a small volume of the microcracks practically does not influence neither average porosity, nor density, but it is quite enough to explain typical experimental data on attenuation. On the other hand, it is clear that near- spherical (cylindrical) pores with much greater volume could significantly change porosity and density. However, in absence of the fluid saturation they practically do not influence the absorption because the cylindrical and spheroidal cavities in a solid matrix are not soft inclusions unlike the thin cracks and similar defects.

Summarizing the discussion it can be stated that the proposed micromechanical model for absorption and elasticity of microinhomogeneous solids is in a good agreement with the main features of elastic wave attenuation/dispersion which are experimentally observed in various microinhomogeneous solids. The obtained functional dependencies also agree well with the best known phenomenological approximations and satisfy the causality principle (Kramers-Kronig relations) unlike some phenomenological models [3, 25, 26], because the discussed results are self- consistently derived from a few basic and intuitively clear physical assumptions about the medium microstructure. Moreover, quantitatively the model also yields rather verisimilar estimates for the absolute values of absorption and dispersion. For more detailed comparison it would be helpful to have available more comprehensive experimental data on the complementary values of attenuations and wave speeds for different types of waves (the shear, bulk longitudinal and Young's modes) in a wide frequency band and at different densities of the microstructural defects (the density of the defects can be changed, for example, by applying a static stress or changing the material temperature).

6. Conclusions

The suggested model of a microinhomogeneous solid allowed for calculation of elastic and dissipative properties of an elastic material containing isotropically oriented highly compliant planar defects. It is shown that by comparison of the initial moduli of an intact matrix material and their values in the microinhomogeneous material it is possible to predict the magnitudes of the near-constant decrements for the corresponding waves without knowing details of dissipative properties of the defects. The model implies a few basic parameters describing the medium microstructure, which allows for obtaining further physical predictions. In this paper, the basic parameters of the microscopic defects were introduced semi-phenomenologically using reasonable physical arguments and taking into account available experimental data. Alternatively, they can be obtained from physical models of microinhomogeneities (for example, from models of crack-like defects [24]) and incorporated into the model of the microinhomogeneous medium to predict its properties "from the first principles".

The model has proven to be in a good functional agreement with main acoustical properties experimentally observed in many microinhomogeneous solids (for example, the linear dependence of the absorption coefficient on frequency) which had no satisfactory physical explanations and were described mostly phenomenologically [3, 25, 26]. Other directions of the development the suggested 3D model are quite evident by analogy with its 1D variants [17, 18, 19, 21, 23] (self-consistently implying dissipation, dispersion, and nonlinearity) and can be considered elsewhere.

Acknowledgement

The work was supported by a grant of the Research Council of the Katholieke Universiteit Leuven. Comments by the reviewers were extremely helpful. Authors are also grateful to Prof. W. Arnold from the Fraunhofer Institute for Nondestructive Testing, who, in particular, stimulated this study by attracting authors' attention to experimental results obtained for nano-crystalline metals.

References

[1] J. B. Walsh: The effect of cracks on the uniaxial elastic compression of rocks. J. Geoph. Res. **70** (1965) 399–411.
[2] J. B. Walsh: The effect of cracks on Poisson's ratio. J. Geoph. Res. **70** (1965) 5249–5247.
[3] S. Y. Kogan: A brief review of seismic wave absorption theories, Pts.1,2. Physics of the Earth (Fizika zemli) **11** (1966) 3–22. (in Russian. Engl. Transl.: Izv. Earth. Phys., 11, (1966), 3-28).
[4] A. V. Nikolaev: Seismic properties of crumbly media. Physics of the Earth, (Fizika zemli) **2** (1967) 23–31. (in Russian).
[5] D. J. Houlomb: Memory, relaxation, and microfracturing in dilatant rock. J. Geoph. Res. **86** (1981) 6235–6248.
[6] M. A. Sadovsky, L. G. Bolkhovitinov, V. E. Pisarenko: On discrete properties of earth rocks. Physics of the Earth, (Fizika zemli) **12** (1982) 23–31. (in Russian).
[7] V. E. Nazarov, L. A. Ostrovsky, I. A. Soustova, A. M. Sutin: Nonlinear acoustics of micro-inhomogeneous media. Physics of the Earth and Planetary Interiors **50** (1988) 65–73.
[8] L. A. Ostrovsky: On nonlinear acoustics of weakly-compressible media. Akust. Zhurn. **34** (1988) 908–913. (Engl. Transl.: Sov. Phys. Acoust.. 34(3), (1988), 523-528).
[9] I. Y. Belyaeva, V. Y. Zaitsev, L. A. Ostrovsky: Nonlinear acousto-elastic properties of granular media. Acoust. Physics **39** (1993) 11–15.
[10] K. Naugolnykh, L. Ostrovsky: Nonlinear wave processes in acoustics. Cambridge University Press, MA, 1998.
[11] A. M. Sutin, V. E. Nazarov: On the Poisson coefficient of crack-containing media. Akust. Zhurn. **42** (1995) 932–934. (Engl. Transl. Acoust. Phys. 42(6), 1995).
[12] V. E. Nazarov, A. M. Sutin: Nonlinear elastic constants of solids with cracks. J. Acoust. Soc. Amer. **102** (1997) 3349–3354.
[13] V. Gusev, C. Glorieux, W. Lauriks, J. Thoen: Nonlinear bulk and surface shear acoustic waves in materials with histeretic and endpoint memory. Phys. Lett. A **232** (1997) 77–86.
[14] V. E. Gusev, W. Lauriks, E. Thoen: Dispersion of nonlinearity, nonlinear dispersion and absorption of sound in micro-

inhomogeneous materials. J. Acoust. Soc. Amer. **103** (1998) 3216–3226.
[15] R. Guyer, P. Johnson: Nonlinear mesoscopic elastisity: Evidence for a new class of materials. Physics Today (April, 1999) 30–36.
[16] M. J. Lang, M. Duarte, W. Arnold: Measurement of elastic and anelastic properties of nanocrystalline metals. Nanostructured Materials **12** (1999) 811–816.
[17] V. Y. Zaitsev: A model of anomalous acoustic nonlinearity of micro-inhomogeneous media. Acoustics Letters **19** (1996) 171–176.
[18] I. Y. Belyaeva, V. Zaitsev: Nonlinear elastic properties of microinhomogeneous hierarchically structured media. Acoust. Physics **43** (1997) 594–599.
[19] I. Y. Belyaeva, V. Y. Zaitsev: The limiting value of the parameter of elastic nonlinearity in structurally inhomogeneous media. Akust. Zhurnal **44** (1998) 731–737. (Engl. Transl.: Acoust. Phys. 44(6), 1998).
[20] V. Y. Zaitsev, V. E. Nazarov: On the frequency-independent acoustic Q-factor of microinhomogeneous media. Acoustics Letters **21** (1997) 11–15.
[21] V. Y. Zaitsev, V. E. Nazarov, A. E. Shul'ga: On dispersive and dissipative properties of microinhomogeneous media. Akust. Zhurnal **46** (2000) (accepted. Engl. Transl.: Acoust. Phys. 46, (2000), in print).
[22] I. Sneddon: Fourier transforms. Pergamon, 1951.
[23] L. D. Landau, E. M. Lifshitz: Theory of elasticity. Pergamon, 1986.
[24] J. C. Savage: Thermoelastic attenuation of elastic waves by cracks. J. Geophys. Research **71** (1966) 3929–3938.
[25] K. Aki, P. G. Richards: Quantitative seismology, Vol.1. W. H. Freeman and Company, San Francisco, 1980.
[26] T. Bourbié, O. Coussy, B. Zinszner: Acoustique des milieux poreux, publications de l'institut française du pétrole. Editions Technip, Paris, 1986.
[27] M. N. Toksöz, D. H. Johnston, A. Timur: Attenuation of seismic waves in dry and saturated rocks: I. Laboratory measurements. Geophysics **44** (1979) 681–690.
[28] M. N. Toksöz, D. H. Johnston, A. Timur: Attenuation of seismic waves in dry and saturated rocks: II. Mechanisms. Geophysics **44** (1979) 691–711.
[29] G. I. Gurevich: A basic feature of the propagation and attenuation of seismic waves. – In: Aspects of Dynamical Theory of Seismic Wave Propagation, Issues VI (1962),VII (1964). Moscow. (in Russian).
[30] H. P. Liu, D. L. Anderson, H. Kanamori: Velocity dispersion due to unelasticity: implications for sismology and mantle composition. Geophys. J. Roy. Astron. Soc. **47** (1976) 41–58.
[31] G. M. Lundquist, V. C. Cormier: Constraints on the absorption band model of Q. J.Geophys. Res. **85** (1980) 5244–5256.
[32] E. Kjartansson: Constant Q-wave propagation and attenuation. J. Geophys. Res. **84** (1979) 4737–4748.
[33] M. Buckingham: Theory of acoustic attenuation, dispersion and pulse propagation in granular materials including marine sediments. J. Acoust. Soc. Amer. **102** (1997) 2579–2596.
[34] M. Buckingham: Theory of compressional and transverse wave propagation in consolidated porous media. J. Acoust. Soc. Amer. **106** (1999) 575–581.
[35] R. J. O'Connell, B. Budiansky: Seismic velocities in dry and saturated cracked solids. J. Geophys. Res. **79** (1974) 5412–5426.
[36] B. Budiansky, R. J. O'Connell: Elastic moduli of a cracked solid. Int. J. Solid Structures **12** (1976) 81–97.
[37] G. M. Mavko, A. Nur: The effect of nonelliptical cracks on compressibility of rocks. J. Geophys. Res. **83** (1978) 4459–4468.
[38] L. Knopoff, G. Mac-Donald: Models for acoustic loss in solids. J. Geophys. Res. **65** (1960) 2191.
[39] J. B. Walsh: Seismic wave attenuation in rock due to friction. J. Geoph. Res. **71** (1966) 2591–2599.
[40] G. M. Mavko: Frictional attenuation: An inherent amplitude dependece. J. Geophys. Res. **84** (1979) 4769–4775.
[41] M. A. Biot: Theory of acoustic attenuation, propagation of elastic waves in a fluid-saturated porous solid. I. Low-frequency range. J. Acoust. Soc. Amer. **28** (1956) 168–178.
[42] M. A. Biot: Theory of propagation of elastic waves in a fluid-saturated porous solid: II. Higher frequency range. J. Acoust. Soc. Amer. **28** (1956) 179–191.
[43] D. H. Johnston: Attenuation: A state-of-the art summary. – In: Seismic wave attenuation. Society of exploration Geophysicists, Tulsa, OK, 1981, 123–135.